Motion coordination algorithms resulting from classical geometric optimization problems

Jorge Cortés

Coordinated Science Laboratory
University of Illinois at Urbana-Champaign
1308 West Main Street, Urbana, Illinois 61801
`http://motion.csl.uiuc.edu/~jorge`
Email: `jcortes@uiuc.edu`

Abstract. This paper introduces various geometric optimization problems and explores their relationship with motion coordination algorithms for networks of mobile agents. For each problem, the objective is the optimization of an appropriate multi-center function encoding the sensing task to be achieved by the mobile network in a dynamic environment. We present five different scenarios: the expected value scenario, the expected value scenario with limited range interactions, the area scenario, the worst-case scenario and the non-interference scenario. We carefully analyze the smoothness properties and gradient information of the multi-center functions. Based on this investigation, we propose distributed motion coordination algorithms specifically tailored for each scenario. The multi-center functions play the role of network aggregate cost functions certifying the validity of the coordination algorithms. Various numerical simulations illustrate the results.

Keywords: Coverage optimization, motion coordination algorithms, geometric optimization, nonsmooth analysis, proximity graphs, Voronoi partitions
AMS subject classification: 37N35, 68W15, 93D20, 49J52, 05B40
PACS numbers: 02.30.Yy, 45.10.Db, 89.70.+c

1. INTRODUCTION

Consider the following scenario: let $(p_1, \ldots, p_n)$ denote the location of n mobile agents in a convex polygonal environment Q. Assume that the agents have the ability to sense its immediate environment, communicate with other agents, process the received data, and plan its own motions accordingly. Furthermore, assume that certain events of interest are taking place in the environment Q that the mobile network has to take care of. How should the mobile network plan its motion in order to optimize the coverage of the environment? More precisely, we aim at designing motion coordination algorithms that, implemented over each mobile agent, will achieve the objective of optimally positioning the agents in the environment with respect to the desired sensing task.

Since the initial works from the graphics and ecology communities on distributed coordination on swarms and flocking [1, 2], the design of coordination algorithms has been studied extensively by the behavioral control and the control theory communities (see [3–10] and references therein). In this paper, we describe an innovative technical approach that relies on non-smooth distributed descent algorithms and on aggregate

utility functions that encode optimal coverage and sensing policies. We introduce various notions of quality-of-service provided by an adaptive mobile network in a dynamic environment. We refer to these notions as multi-center functions. We set up five different geometric optimization problems: the expected value scenario, the expected value scenario with limited range interactions, the area scenario, the worst-case scenario and the non-interference scenario. We carefully investigate the smoothness properties and the (generalized) gradient information of the multi-center functions. Building on this analysis, we design coordination algorithms implementable by a mobile network with sensing, communication and motion capabilities that optimize the multi-center functions.

When designing motion coordination algorithms, we take into careful consideration all constraints present on the mobile network. In particular, the coordination algorithms should be: (i) adaptive, in order to provide the network with the ability to address changing environments, sensing task, and network topology (due to agents departures, arrivals, or failures); (ii) distributed, in the sense that the behavior of each agent depends only on the location of its neighbors. They should typically not require a fixed-topology communication graph, i.e., allow for the neighborhood relationships to change as the network evolves. The advantages of distributed algorithms are scalability and robustness; (iii) verifiable asymptotically correct, i.e., guarantee monotonic optimization of the cost function encoding the sensing task. Asymptotically, the evolution of the mobile network should be guaranteed to converge to the critical points of the optimal sensor coverage problem. The importance of formal verification proofs increases with the dimension and complexity of vehicle networks; and (iv) amenable to asynchronous implementation, meaning that the algorithms should be implementable in a network composed of agents evolving at different speeds, with different computation and communication capabilities. In such a case, no global synchronization is required and convergence properties are preserved even if information about neighboring vehicles propagates with some delay.

The organization of the paper is as follows. In Section 2, we introduce some basic concepts from computational geometry [11, 12] and present the model of synchronous mobile network considered throughout the paper. Section 3 introduces various geometric optimization problems in which service sites are spatially allocated to fulfill a specified request [13–16]. We propose different notions of quality-of-service to measure the network performance, depending on the specific sensing task, the capabilities of the agents and the information about the distribution of events taking place in the environment. We state the differentiable properties of these functions and the expressions of their (generalized) gradients via nonsmooth analysis [17]. We show that their critical points are *center Voronoi configurations*. Finally, Section 4 presents distributed motion coordination algorithms for each of the scenarios introduced in Section 3. Using the stability tools in [18–20], we propose novel strategies based on the nonsmooth generalized gradients of the aggregate cost functions. We investigate their asymptotic behavior and show that the algorithms are guaranteed to continuously improve the corresponding network performance measure. A detailed analysis of all results presented in this paper can be found in [7, 21, 22].

2. PRELIMINARIES

Let $\|\cdot\|$ denote the Euclidean distance function on $\mathbb{R}^N$, $N \in \mathbb{N}$, and let $v \cdot w$ denote the scalar product of $v, w \in \mathbb{R}^N$. Let versus(v) denote the unit vector in the direction of $0 \neq v \in \mathbb{R}^N$, i.e., versus$(v) = v/\|v\|$. Given $S \subset \mathbb{R}^N$, co(S) and int$S$ denote its convex hull and interior set, respectively. Let $1_S : \mathbb{R}^N \to \{0,1\}$ be the indicator function defined by $1_S(q) = 1$ if $q \in S$, and $1_S(q) = 0$ if $q \notin S$. If S is convex, let $\mathrm{proj}_S \colon \mathbb{R}^N \to S$ denote the orthogonal projection onto S and let $\mathrm{D}_S \colon \mathbb{R}^N \to \mathbb{R}$ denote the distance function to S. For $p \in \mathbb{R}^N$ and $r \in \mathbb{R}_+ = [0, +\infty)$, let $B_r(p) = \{q \in \mathbb{R}^N \mid \|q - p\| \leq r\}$ denote the closed ball in $\mathbb{R}^N$ centered at p of radius r. Let $n_{B_r(p)}(q)$ denote the unit outward normal to $B_r(p)$ at $q \in \partial B_r(p)$.

Let Q be a simple convex polygon in $\mathbb{R}^2$. We denote by $\mathrm{Ed}(Q) = \{e_1, \ldots, e_M\}$ and $\mathrm{Ve}(Q) = \{v_1, \ldots, v_L\}$ the set of edges and vertices of Q, respectively. If $e \in \mathrm{Ed}(Q)$, we let n_e denote the unit normal to e pointing toward int(Q). The *diameter of* Q is defined as $\mathrm{diam}(Q) = \max_{q,p \in Q} \|q - p\|$. Let $P = (p_1, \ldots, p_n) \in Q^n \subset (\mathbb{R}^2)^n$ denote the location of n generators in Q.

2.1. Voronoi partitions and proximity graphs

In this section, we review the notion of Voronoi partition generated by sets of points on the Euclidean plane; we refer the reader to [11, 12] for comprehensive treatments. Next, we shall present some relevant concepts on proximity graph functions. This notion is an extension of the notion of proximity graph as explained in the survey article [23].

A *covering* of $\mathbb{R}^2$ is a collection of subsets of $\mathbb{R}^2$ whose union is $\mathbb{R}^2$; a *partition* of $\mathbb{R}^2$ is a covering whose subsets have disjoint interiors. Let $\mathscr{P}$ be a set of n distinct points $\{p_1, \ldots, p_n\}$ in $\mathbb{R}^2$. The *Voronoi partition of* $\mathbb{R}^2$ generated by $\mathscr{P}$ with respect to the Euclidean norm is the collection of sets $\{V_i(\mathscr{P})\}_{i \in \{1,\ldots,n\}}$ defined by

$$V_i(\mathscr{P}) = \{q \in \mathbb{R}^2 \mid \|q - p_i\| \leq \|q - p_j\|, \text{ for all } p_j \in \mathscr{P}\}.$$

It is customary and convenient to refer to $V_i(\mathscr{P})$ as V_i. The boundary of each set V_i is the union of a finite number of segments and rays. A vertex $v \in \mathrm{Ve}(V_i(P))$ is *nondegenerate* if it is determined by exactly three elements. Otherwise it is *degenerate*. The configuration P is *nondegenerate* if all its vertices are nondegenerate, otherwise it is *degenerate*.

Let Σ_n be the set of permutations of n elements. A map $f \colon X^n \to 2^{X \times X}$ is Σ_n-*equivariant* if for all $(x_1, \ldots, x_n) \in X^n$ and $\sigma \in \Sigma_n$, $(x_i, x_j) \in f(x_1, \ldots, x_n)$ implies $(x_{\sigma(i)}, x_{\sigma(j)}) \in f(x_{\sigma(1)}, \ldots, x_{\sigma(n)})$. A *proximity graph function* associates to a set of n distinct points $\mathscr{P} = \{p_1, \ldots, p_n\}$ in $\mathbb{R}^2$ a graph with vertex set $\mathscr{P}$ and edge set $\mathscr{E}(p_1, \ldots, p_n)$, where $\mathscr{E} \colon (\mathbb{R}^2)^n \to 2^{\mathbb{R}^2 \times \mathbb{R}^2}$ is a Σ_n-equivariant map with the property that $\mathscr{E}(p_1, \ldots, p_n) \subseteq \mathscr{P}^2 = \{p_1, \ldots, p_n\}^2 = \{p_1, \ldots, p_n\} \times \{p_1, \ldots, p_n\}$. Note that, since the map $\mathscr{E}$ is Σ_n-equivariant, the value of $\mathscr{E}(p_1, \ldots, p_n)$ is independent of the ordering of the elements $(p_1, \ldots, p_n)$, and therefore, we will write it as $\{p_1, \ldots, p_n\} = \mathscr{P} \mapsto \mathscr{E}(\mathscr{P})$, and refer to it as the *proximity edge function* corresponding to the proximity graph function

$\mathscr{P} \mapsto \mathscr{G}(\mathscr{P})$. To each proximity graph function $\mathscr{G}$, one can associate the *set of neighbors map* $\mathscr{N}_{\mathscr{G}} \colon \mathbb{R}^2 \times 2^{\mathbb{R}^2} \to 2^{\mathbb{R}^2}$, defined by $\mathscr{N}_{\mathscr{G}}(p, \mathscr{P}) = \{q \in \mathscr{P} \mid (p,q) \in \mathscr{E}_{\mathscr{G}}(\mathscr{P})\}$. We will often write $\mathscr{N}_{\mathscr{G},p}(\mathscr{P})$ to denote $\mathscr{N}_{\mathscr{G}}(p, \mathscr{P})$. For $r \in \mathbb{R}_+$, we have the following proximity graph functions:

(i) the *Delaunay graph* $\mathscr{P} \mapsto \mathscr{G}_{\mathrm{D}}(\mathscr{P}) = (\mathscr{P}, \mathscr{E}_{\mathrm{D}}(\mathscr{P}))$ with edge set

$$\mathscr{E}_{\mathrm{D}}(\mathscr{P}) = \{(p_i, p_j) \in \mathscr{P}^2 \setminus \mathrm{diag}(\mathscr{P}^2) \mid V_i(\mathscr{P}) \cap V_j(\mathscr{P}) \neq \emptyset\};$$

(ii) the *r-disk graph* $\mathscr{P} \mapsto \mathscr{G}_{\mathrm{disk}}(\mathscr{P}, r) = (\mathscr{P}, \mathscr{E}_{\mathrm{disk}}(\mathscr{P}, r))$ with edge set

$$\mathscr{E}_{\mathrm{disk}}(\mathscr{P}, r) = \{(p_i, p_j) \in \mathscr{P}^2 \setminus \mathrm{diag}(\mathscr{P}^2) \mid \|p_i - p_j\| \leq r\};$$

(iii) the *r-limited Delaunay (or, limited-range Delaunay) graph* $\mathscr{P} \mapsto \mathscr{G}_{\mathrm{LD}}(\mathscr{P}, r) = (\mathscr{P}, \mathscr{E}_{\mathrm{LD}}(\mathscr{P}, r))$ consists of the edges $(p_i, p_j) \in \mathscr{P}^2 \setminus \mathrm{diag}(\mathscr{P}^2)$ with the property

$$\big(V_i(\mathscr{P}) \cap B_{\frac{r}{2}}(p_i)\big) \cap \big(V_j(\mathscr{P}) \cap B_{\frac{r}{2}}(p_j)\big) \neq \emptyset. \tag{1}$$

There are other important proximity graphs such as the Gabriel graph or the Euclidean Minimum Spanning Tree. We refer to [22, 23] for further details.

Note that in the previous definitions we have emphasized the fact that the points $\{p_1, \ldots, p_n\}$ are distinct. Occasionally though, we will consider ordered sets of possibly coincident points. In this case, it is useful to adopt the following notation: given a tuple $(p_1, \ldots, p_n) \in (\mathbb{R}^2)^n$, we let $\{p_1, \ldots, p_n\}$, or equivalently $\mathscr{P}$, denote the associated point set that only contains the corresponding distinct points. The cardinality of $\mathscr{P} = \{p_1, \ldots, p_n\}$ is less than or equal to n. More precisely, if $\mathscr{S}$ denotes the set

$$\mathscr{S} = \{(p_1, \ldots, p_n) \in (\mathbb{R}^2)^n \mid p_i = p_j \text{ for some } i, j \in \{1, \ldots, n\}, i \neq j\}, \tag{2}$$

then $\#\mathscr{P} < n$ if $(p_1, \ldots, p_n) \in \mathscr{S}$ and $\#\mathscr{P} = n$ if $(p_1, \ldots, p_n) \notin \mathscr{S}$. The *Voronoi covering* $\mathscr{V}(p_1, \ldots, p_n) = \{V_i(p_1, \ldots, p_n)\}_{i \in \{1, \ldots, n\}}$ *generated by the tuple* $(p_1, \ldots, p_n)$ is defined by assigning to each point p_i its corresponding Voronoi cell in the Voronoi partition generated by $\mathscr{P}$. Note that coincident points in the tuple $(p_1, \ldots, p_n)$ have the same Voronoi cell.

We are now in a position to discuss distributed control laws and algorithms in formal terms. Let $\mathscr{G}$ be a proximity graph function and let Y be a set. A map $f \colon (\mathbb{R}^2)^n \to Y^n$ is *spatially distributed over* $\mathscr{G}$ if there exist maps $\tilde{f}_i \colon \mathbb{R}^2 \times 2^{(\mathbb{R}^2)^n} \to Y$, $i \in \{1, \ldots, n\}$, with the property that for all $(p_1, \ldots, p_n) \in (\mathbb{R}^2)^n$

$$f_i(p_1, \ldots, p_n) = \tilde{f}_i(p_i, \{p_j \in \mathbb{R}^2 \mid p_j \in \mathscr{N}_{\mathscr{G},p_i}(\mathscr{P})\}),$$

where f_i denotes the ith-component of f. A vector field X on $(\mathbb{R}^2)^n$ is *spatially distributed over* $\mathscr{G}$ if its associated map $X \colon (\mathbb{R}^2)^n \to (\mathbb{R}^2)^n$, where the canonical identification between the tangent space of $(\mathbb{R}^2)^n$ and $(\mathbb{R}^2)^n$ itself is understood, is spatially distributed in the above sense. In other words, to compute the ith component of a spatially-distributed function or vector field at $(p_1, \ldots, p_n)$, it is only required the knowledge of the vertex p_i and the neighboring vertexes in the proximity graph $\mathscr{G}(\{p_1, \ldots, p_n\})$.

One can prove that r-limited Delaunay graph is spatially distributed over $\mathcal{G}_{\text{disk}}(r)$. More precisely, for $r \in \mathbb{R}_+$, the map $\mathcal{N}_{\mathcal{G}_{\text{LD}}(\cdot,r)} : (\mathbb{R}^2)^n \to \left[2^{(\mathbb{R}^2)^n}\right]^n$, defined by

$$(p_1, \ldots, p_n) \mapsto (\mathcal{N}_{\mathcal{G}_{\text{LD}}(r),p_1}(\mathcal{P}), \ldots, \mathcal{N}_{\mathcal{G}_{\text{LD}}(r),p_n}(\mathcal{P})),$$

is spatially distributed over $\mathcal{G}_{\text{disk}}(r)$. Loosely speaking, this proposition states that the r-limited Delaunay graph $\mathcal{G}_{\text{LD}}$ can be computed in a spatially localized way: each agent needs to know only the location of all other agents in a disk of radius r.

2.2. Modeling a network of mobile agents

Here, we introduce the notions of *mobile agent* and of *network of mobile agents*. Let n be the number of agents in the network. Each agent has the following sensing, computation, communication, and motion control capabilities. The ith agent has a processor with the ability of allocating continuous and discrete states and performing operations on them. The ith agent occupies a location $p_i \in Q \subset \mathbb{R}^2$ and it is capable of moving in space, at any time $t \in \mathbb{R}_+$ according to a first order continuous dynamics of the form

$$\dot{p}_i(t) = u_i. \tag{3}$$

Here, the control u_i takes values in a bounded subset of $\mathbb{R}^2$. The processor has access to the agent's location p_i and determines the *control* u_i. The processor of the ith agent is capable of transmitting information to any other agent within a closed disk of radius $r_i \in \mathbb{R}_+$. We will consider two different sensing and communication models: in the first one, we assume that the communication radius r_i is a quantity controllable by the ith processor; in the second one, we assume that the communication radius r_i is a fixed quantity and equal for all agents, $r_i = r \in \mathbb{R}_+$, $i \in \{1, \ldots, n\}$. In both models, the communication bandwidth is assumed to be limited. Throughout the paper, we shall specify the concrete communication model used.

Equivalently, we shall consider groups of mobile agents without communication capabilities, but instead capable of measuring the relative position of each other agent within a closed disk of radius $r_i \in \mathbb{R}_+$. We assume that all communication between agents and all sensing of agents locations are accurate. Note that this network model is synchronous. We refer the reader to [7, 10, 24] for various asynchronous network models.

3. MULTI-CENTER FUNCTIONS AS NETWORK PERFORMANCE MEASURES

In this section, we begin by introducing the precise notions of quality-of-service provided by the mobile network in a dynamic environment. These notions will be later the criteria to judge the asymptotic correctness and performance of the motion coordination algorithms. We end the section by characterizing the smoothness properties of the multi-center functions.

Expected value scenario

Assume that a certain density function $\phi : Q \to \mathbb{R}_+$ is known, describing the probability distribution in Q of the events of interest. Assume further that the mobile agents can control and tune their communication radius (respectively their sensing radius). In such a case, the network tries to minimize the expected distance from any event in the environment to one of the mobile agents of the network (since, because of noise and loss of resolution, the closest agent will be the one which is able to take the best possible measurement of that event or can reach its location more quickly). Accordingly, we set up the following geometric optimization problem

$$\text{minimize}_{p_1,\dots,p_n \in Q} \quad \left\{ \mathscr{H}_{\text{C}}(p_1,\dots,p_n) = \int_Q \min_{i\in\{1,\dots,n\}} \|q-p_i\|^2 \phi(q) dq \right\}. \tag{4}$$

This problem is referred to as the p-median problem in [15]. On $Q^n \setminus \mathscr{S}$, $\mathscr{H}_{\text{C}}$ reads

$$\mathscr{H}_{\text{C}}(P) = \sum_{i=1}^{n} \int_{V_i} \|q-p_i\|^2 \phi(q) dq\,.$$

Given a polytope W in $\mathbb{R}^N$, its centroid, CM_W, is the center of mass of W with respect to the density function ϕ, i.e.,

$$\text{CM}_W = \frac{1}{\text{M}_W} \int_W q\phi(q) dq\,, \quad \text{M}_W = \int_W \phi(q) dq\,.$$

Centroidal Voronoi configurations satisfy $p_i = \text{CM}_{V_i(P)}$ for all $i \in \{1,\dots,n\}$.

We can slightly modify the previous scenario to set up a different geometric optimization problem. If, under the same hypothesis, the mobile agents have a fixed (and common) communication radius $r \in \mathbb{R}_+$ (respectively sensing radius), then the problem turns out to be harder. The objective is still to solve the optimization in equation (4), but now the agents can only communicate to or sense other agents and events up to a fixed distance. We refer to it as the *expected value scenario with range-limited interactions*. To deal with this situation, we introduce the multi-center function

$$\mathscr{H}_{\frac{r}{2}}(p_1,\dots,p_n) = \int_Q \max_{i\in\{1,\dots,n\}} \left(\|q-p_i\|^2 \, 1_{B_{\frac{r}{2}}(p_i)}(q) + \text{diam}(Q)^2 \cdot 1_{Q\setminus B_{\frac{r}{2}}(p_i)}(q) \right) \phi(q) dq,$$

where we assume $r \leq 2\,\text{diam}(Q)$ (since otherwise $Q \subset B_{\frac{r}{2}}(p_i)$ for all $i \in \{1,\dots,n\}$, and the setting would be the same as in the expected value scenario). The factor $1/2$ multiplying the radius comes out of technical reasons. There are two arguments to explain why this function is important to deal with this scenario. The first one is given by the following constant-factor approximation of the value of $\mathscr{H}_{\text{C}}$ (cf. [22]),

$$\mathscr{H}_{\frac{r}{2}}(P) \geq \mathscr{H}_{\text{C}}(P) \geq \beta\, \mathscr{H}_{\frac{r}{2}}(P) > 0\,, \tag{5}$$

for all $P \in Q^n$, and for $\beta = \left(\frac{r}{2\,\text{diam}(Q)}\right)^2 \in [0,1]$. That is, the optimization of $\mathscr{H}_{\frac{r}{2}}$ is equivalent, to the extent determined by equation (5), to the optimization of $\mathscr{H}_{\text{C}}$. The second reason is related with the gradient of $\mathscr{H}_{\frac{r}{2}}$. We postpone its exposition to Section 4.

Area scenario

An alternative optimization problem is the area scenario. Assuming that the mobile agents have a fixed finite communication (respectively, sensing) radius $r \in \mathbb{R}_+$, the mobile network should maximize the amount of area of the environment covered. If a distribution density function $\phi : Q \to \mathbb{R}_+$ is known, then the area can be weighted accordingly. The following geometric optimization problem describes this scenario:

$$\text{maximize}_{p_1,\ldots,p_n \in Q} \quad \left\{ \mathscr{H}_{\text{area}}(p_1,\ldots,p_n) = \int_Q \left(\max_i \, 1_{B_{\frac{r}{2}}(p_i)}(q) \right) \phi(q) dq \right\}.$$

Worst-case scenario

Assume now that no information is available about the distribution of events taking place in the environment. Assume further that the mobile agents can control and tune their communication radius (respectively their sensing radius). Since no information is available, it seems reasonable to consider the *worst-case scenario*, that is, that the event of interest will occur at the furthest-away point from the network in the environment. Therefore, the network tries to minimize the largest possible distance from any point in the domain to one of the agent locations,

$$\text{minimize}_{p_1,\ldots,p_n \in Q} \quad \left\{ \mathscr{H}_{\text{DC}}(p_1,\ldots,p_n) = \max_{q \in Q} \left(\min_{i \in \{1,\ldots,n\}} \|q - p_i\| \right) \right\}.$$

This problem is referred to as the p-center problem in [15, 25]. In terms of the Voronoi partition, the function $\mathscr{H}_{\text{DC}}$ admits the following alternative expression

$$\mathscr{H}_{\text{DC}}(P) = \max_{i \in \{1,\ldots,n\}} \left\{ \max_{q \in V_i} \|q - p_i\| \right\}.$$

It is conjectured in [25] that the p-center problem can be restated as a disk-covering problem: how to cover a region with disks of minimum radius, which reads

$$\min\{R \mid \ \cup_{i \in \{1,\ldots,n\}} B(p_i, R) \supseteq Q\}.$$

In Theorem 3.2 we provide a positive answer to this question. Given a polytope W in $\mathbb{R}^N$, its circumcenter, CC_W, is the center of the minimum-radius sphere that contains W. We say that P is a *circumcenter Voronoi configuration* if $p_i = \text{CC}_{V_i(P)}$, for all $i \in \{1,\ldots,n\}$.

Non-interference scenario

The objective here is to maximize the coverage of the domain in such a way that the various sensing radius do not overlap or leave the environment (because of interference). In this situation, the network tries to solve the following geometric optimization problem

$$\text{maximize}_{p_1,\ldots,p_n \in Q} \quad \left\{ \mathscr{H}_{\text{SP}}(p_1,\ldots,p_n) = \min_{i \neq j \in \{1,\ldots,n\}} \left(\tfrac{1}{2}\|p_i - p_j\|, \text{D}(p_i, \partial Q) \right) \right\},$$

so that each agent can fi t a circular sensing region as large as possible within the environment and without overlapping with the regions belonging to other agents. In terms of the Voronoi partition, the function $\mathscr{H}_{\mathrm{SP}}$ admits the following alternative expression

$$\mathscr{H}_{\mathrm{SP}}(P) = \min_{i\in\{1,\dots,n\}} \left\{ \min_{q\notin \mathrm{int}\, V_i} \|q-p_i\| \right\}.$$

A similar conjecture to the one presented above is that this problem can be restated as a sphere-packing problem: how to maximize the coverage of a region with non-overlapping disks (contained in the region) of minimum radius. The problem reads:

$$\max\{R \mid \ \cup_{i\in\{1,\dots,n\}} B_2(p_i,R) \subseteq Q,\ \mathrm{int}(B(p_i,R)) \cap \mathrm{int}(B(p_j,R)) = \emptyset\}.$$

In Theorem 3.2 we provide a positive answer to this question. Given a polytope W in $\mathbb{R}^N$, its incenter set, IC_W, is the set of the centers of maximum-radius spheres contained in W. We say that $P \in Q^n$ is an *incenter Voronoi configuration* if $p_i \in \mathrm{IC}_{V_i(P)}$, for all $i \in \{1,\dots,n\}$. If P is an incenter Voronoi confi guration, and each Voronoi region $V_i(P)$ has a unique incenter, $\mathrm{IC}_{V_i(P)} = \{p_i\}$, then P is a *generic incenter Voronoi configuration*.

Smoothness analysis of the multi-center functions

The following discussion gathers the results concerning the smoothness properties of the multi-center functions introduced above. The proof of the following result is based on a generalized statement of the Conservation-Of-Mass Lemma. For further details, the reader is referred to [22] and references therein.

Theorem 3.1 *The multi-center functions $\mathscr{H}_C$, $\mathscr{H}_{\frac{r}{2}}$ and $\mathscr{H}_{area}$ are globally Lipschitz on Q^n, and continuously differentiable on $Q^n \setminus \mathscr{S}$, where for each $i \in \{1,\dots,n\}$*

$$\begin{aligned}
\frac{\partial \mathscr{H}_C}{\partial p_i}(P) &= \int_{V_i} \frac{\partial}{\partial p_i}\|q-p_i\|^2 \phi(q) dq = 2\,\mathrm{M}_{V_i(P)}(p_i - \mathrm{CM}_{V_i(P)}),\\
\frac{\partial \mathscr{H}_{\frac{r}{2}}}{\partial p_i}(P) &= 2\,\mathrm{M}_{V_i(P)\cap B_{\frac{r}{2}}(p_i)}(p_i - \mathrm{CM}_{V_i(P)\cap B_{\frac{r}{2}}(p_i)})\\
&\qquad + \left(\left(\frac{r}{2}\right)^2 - \mathrm{diam}(Q)^2\right) \sum_{k=1}^{M_i(r)} \int_{\mathrm{arc}_{i,k}(r)} n_{B_{\frac{r}{2}}(p_i)}\, \phi,\\
\frac{\partial \mathscr{H}_{area}}{\partial p_i}(P) &= \sum_{k=1}^{M_i(r)} \int_{\mathrm{arc}_{i,k}(r)} n_{B_{\frac{r}{2}}(p_i)}\, \phi.
\end{aligned}$$

with $\mathrm{arc}_{i,k}(r)$, $k \in \{1,\dots,M_i(r)\}$ *the arcs in the boundary of* $V_i(P) \cap B_{\frac{r}{2}}(p_i)$. *As a consequence, the critical points of $\mathscr{H}_C$ are centroidal Voronoi configurations.*

Concerning the smoothness properties of the multi-center functions $\mathscr{H}_{\mathrm{DC}}$ and $\mathscr{H}_{\mathrm{SP}}$, let us consider the following alternative expressions. Let

$$\mathscr{H}_{\mathrm{DC}}(P) = \max_{i\in\{1,\dots,n\}} G_i(P)\,, \quad \mathscr{H}_{\mathrm{SP}}(P) = \min_{i\in\{1,\dots,n\}} F_i(P)\,,$$

where $G_i(P) = \max_{q\in V_i(P)} \|q-p_i\|$ and $F_i(P) = \min_{q\notin \operatorname{int} V_i(P)} \|q-p_i\|$. For a convex polygon $W\subset\mathbb{R}^2$, defi ne the functions

$$\begin{aligned}\lg_W(p) &= \max\{\|q-p\| \mid\ q\in W\} = \max\{\|v-p\| \mid\ v\in \mathrm{Ve}(W)\}\,,\\ \mathrm{sm}_W(p) &= \min\{\|q-p\| \mid\ q\notin \operatorname{int}(W)\} = \min\{\mathrm{D}_e(p) \mid\ e\in \mathrm{Ed}(W)\}\,.\end{aligned}$$

These functions are locally Lipschitz and regular (the reader is referred to [17] for a comprehensive treatment of nonsmooth analysis), and their generalized gradients are given by $\partial \lg_Q(p) = \mathrm{co}\{\mathrm{versus}(p-v) \mid\ v\in \mathrm{Ve}(Q)\,,\ \lg_Q(p) = \|p-v\|\}$ and $\partial \mathrm{sm}_Q(p) = \mathrm{co}\{n_e \mid\ e\in \mathrm{Ed}(Q)\,,\ \mathrm{sm}_Q(p) = \mathrm{D}_e(p)\}$. Note that $G_i(P) = \lg_{V_i(P)}(p_i)$ and $F_i(P) = \mathrm{sm}_{V_i(P)}(p_i)$. Despite the slight abuse of notation, it is convenient to let $\partial \lg_{V_i(P)}(p_i)$ denote $\partial \lg_V(p_i)_{|V=V_i(P)}$, and let $\partial \mathrm{sm}_{V_i(P)}(p_i)$ denote $\partial \mathrm{sm}_V(p_i)_{|V=V_i(P)}$, i.e., holding fi xed the Voronoi cell V_i.

The properties of the functions G_i and F_i are strongly affected by the dependence on the Voronoi partition $\mathscr{V}(P)$. These properties can be fully characterized (the interested reader is referred to [21] for a detailed discussion): indeed, both $G_i, -F_i : Q^n \to \mathbb{R}$ are locally Lipschitz and regular, and their generalized gradients can be described in a precise way by means of a careful analysis of the vertexes and edges where their values are attained, and of the degenerate/nondegenerate character of the Voronoi partition. In the sake of brevity, here we will only highlight the fact that the knowledge of the generalized gradients of G_i and F_i is key to describe the generalized gradients of the functions $\mathscr{H}_{\mathrm{DC}}$ and $\mathscr{H}_{\mathrm{SP}}$, as we do next.

Theorem 3.2 *The multi-center functions $\mathscr{H}_{DC}, -\mathscr{H}_{SP} : Q^n \to \mathbb{R}$ are locally Lipschitz and regular. Their generalized gradients can be expressed as*

$$\begin{aligned}\partial \mathscr{H}_{DC}(P) &= \mathrm{co}\{\partial G_i(P) \mid\ i \text{ such that } G_i(P) = \mathscr{H}_{DC}(P)\}\,,\\ \partial \mathscr{H}_{SP}(P) &= \mathrm{co}\{\partial F_i(P) \mid\ i \text{ such that } F_i(P) = \mathscr{H}_{SP}(P)\}\,.\end{aligned}$$

Moreover,

- *(i) if $P\in Q^n$ is nondegenerate and $0\in \operatorname{int}\partial\mathscr{H}_{DC}(P)$, then P is a strict local minimum of $\mathscr{H}_{DC}$, all generators verify $G_i(P) = \mathscr{H}_{DC}(P)$ and P is a circumcenter Voronoi configuration;*
- *(ii) if $P\in Q^n$ and $0\in \operatorname{int}\partial\mathscr{H}_{SP}(P)$, then P is a strict local maximum of $\mathscr{H}_{SP}$, all generators verify $F_i(P) = \mathscr{H}_{SP}(P)$ and P is a generic incenter Voronoi configuration.*

Remark 3.3 Theorem 3.2(i) and (ii) provide the interpretation of the multi-center problems given at the beginning of this section: since all generators are active, they share the same radius.

4. MOTION COORDINATION ALGORITHMS

In this section, we develop continuous-time implementations of the gradient ascent for the multi-center functions introduced in the previous section. Recall that the agents' location obeys a first order dynamical behavior, as described in equation (3).

We start by considering the multi-center functions $\mathscr{H}_{\mathrm{C}}$, $\mathscr{H}_{\frac{r}{2}}$ and $\mathscr{H}_{\mathrm{area}}$. Building on the result of Theorem 3.1, pick one of the multi-center functions as an aggregate objective cost to be optimized and impose that the location p_i follows its gradient flow. In more precise terms, we set up the following control laws defined over the set $Q^n \setminus \mathscr{S}$

$$u_i = -\frac{\partial \mathscr{H}_{\mathrm{C}}}{\partial p_i}(P) = 2\,\mathrm{M}_{V_i(P)}(\mathrm{CM}_{V_i(P)} - p_i)\,, \tag{6a}$$

$$\begin{aligned} u_i = -\frac{\partial \mathscr{H}_{\frac{r}{2}}}{\partial p_i}(P) &= 2\,\mathrm{M}_{V_i(P)\cap B_{\frac{r}{2}}(p_i)}(\mathrm{CM}_{V_i(P)\cap B_{\frac{r}{2}}(p_i)} - p_i) \\ &\quad + \Big(\mathrm{diam}(Q)^2 - \Big(\frac{r}{2}\Big)^2\Big) \sum_{k=1}^{M_i(r)} \int_{\mathrm{arc}_{i,k}(r)} n_{B_{\frac{r}{2}}(p_i)}\,\phi\,, \end{aligned} \tag{6b}$$

$$u_i = \frac{\partial \mathscr{H}_{\mathrm{area}}}{\partial p_i}(P) = \sum_{k=1}^{M_i(r)} \int_{\mathrm{arc}_{i,k}(r)} n_{B_{\frac{r}{2}}(p_i)}\,, \tag{6c}$$

where we assume that the partition $\mathscr{V}(P) = \{V_1, \ldots, V_n\}$ is continuously updated. One can prove the following result.

Proposition 4.1 *Consider the gradient dynamical system on $Q^n \setminus \mathscr{S}$ defined by equation* (6) *for each of the multi-center functions $\mathscr{H}_C$, $\mathscr{H}_{\frac{r}{2}}$ and $\mathscr{H}_{area}$. Then, we have*

(i) The gradient dynamical system (6a) *is spatially distributed over the Delaunay graph $\mathscr{G}_{\mathrm{D}}$, and the gradient dynamical systems* (6b) *and* (6c) *are spatially distributed over the r-limited Delaunay graph $\mathscr{G}_{\mathrm{LD}}(r)$.*

(ii) For each of the flows in (6)*, the agents' location evolution starting at $P_0 \in Q^n \setminus \mathscr{S}$ remains in $Q^n \setminus \mathscr{S}$ and converges asymptotically to the set of critical points of the corresponding aggregate objective function. Assuming this set is finite, the agents' location converges to a single critical point.*

Remark 4.2 Note that the gradient ascent is not guaranteed to find the global optimum. For example, in the vector quantization literature, it is known that for "bimodal" distribution density functions, the solution to the gradient flow reaches local maxima where the number of agents allocated to the two region of maxima are not optimally partitioned.

We are now in a position to recover the discussion about the expected value scenario with range-limited interactions that we began in Section 3. There, we introduced the function $\mathscr{H}_{\frac{r}{2}}$ to deal with this situation. One of the reasons that we gave was the constant-factor approximation (5) of the value of $\mathscr{H}_{\mathrm{C}}$. The other reason is given by Proposition 4.1(i). The gradient flow of $\mathscr{H}_{\mathrm{C}}$ is spatially distributed over the Delaunay graph $\mathscr{G}_{\mathrm{D}}$, and, therefore, not generally implementable over a network of mobile agents

with a fixed (and common) communication radius $r \in \mathbb{R}_+$ (respectively sensing radius). On the other hand, the gradient flow of $\mathscr{H}_{\frac{r}{2}}$ is spatially distributed over the r-limited Delaunay graph $\mathscr{G}_{\mathrm{LD}}(r)$, and therefore can be implemented over networks of mobile agents with fixed radius r.

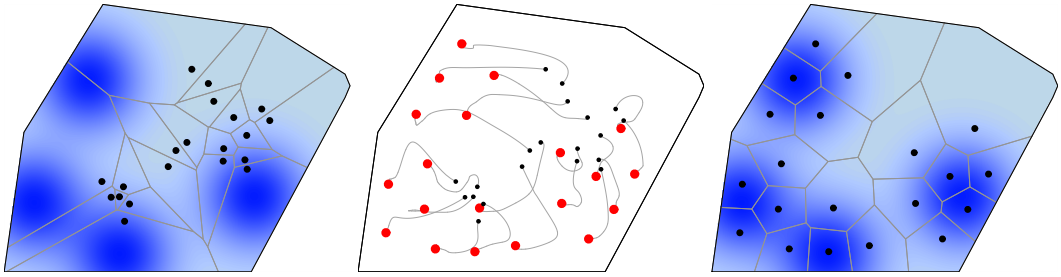

FIGURE 1. Expected value scenario: continuous-time algorithm (6a) for 20 mobile agents in the convex polygonal environment defined by the vertexes of coordinates $\{(0,0),(2.125,0),(2.9325,1.5),(2.975,1.6),(2.9325,1.7),(2.295,2.1),(0.85,2.3),(0.17,1.2)\}$ (in meters). The density function ϕ is the sum of four Gaussian functions of the form $11\exp(6(-(x-x_{\mathrm{center}})^2-(y-y_{\mathrm{center}})^2))$ and is represented by means of its contour plot. The centers $(x_{\mathrm{center}},y_{\mathrm{center}})$ of the Gaussians are given by $(2.15,.75)$, $(1.,.25)$, $(.725,1.75)$ and $(.25,.7)$, respectively. The left (respectively, right) figure illustrates the initial (respectively, final) locations and Voronoi partition. The central figure illustrates the gradient descent flow. After 13 seconds, the value of the multi-center function is approximately .515.

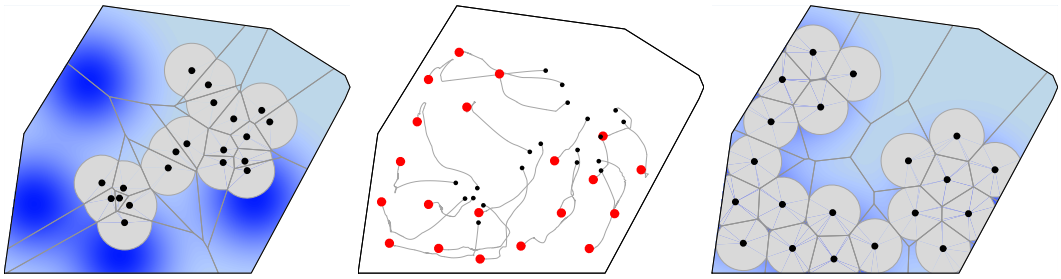

FIGURE 2. Expected value scenario with range-limited interactions: continuous-time algorithm (6b) for 20 mobile agents in the same convex polygonal environment and with the same density function ϕ as in Figure 1. Each agent operates with a finite sensing/communication radius equal to $r = .47$. The left (respectively, right) figure illustrates the initial (respectively, final) locations and Voronoi partition. The central figure illustrates the gradient ascent flow. For each agent i, the intersection $V_i \cap B_{\frac{r}{2}}(p_i)$ is plotted in light gray. After 13 seconds, the value of the multi-center function is approximately 4.794. From the constant-factor approximation (5), we compute $\beta \approx 0.00484$, where P_{final} denotes the final configuration in Figure 2. The absolute error is guaranteed to be less than or equal to $(1-\beta)\mathscr{H}_{\frac{r}{2}}(P_{\mathrm{final}}) \approx 4.77$. In order to compare the performance of this execution with the performance of the algorithm in the expected value scenario (cf. Figure 1), we compute the percentage error in the value of the multi-center function $\mathscr{H}_{\mathrm{C}}$ at their final configurations. This percentage error is approximately equal to 3.277%. As expected, we verified in simulations that the percentage error of the performance of the limited-range implementation improves with higher values of the ratio $r/\operatorname{diam}(Q)$.

Let us consider now the worst-case scenario and the non-interference scenario. Consider the (signed) generalized gradient flow for the multi-center functions $\mathscr{H}_{\mathrm{DC}}$ and $\mathscr{H}_{\mathrm{SP}}$,

$$\dot{P} = -\operatorname{Ln}(\partial\mathscr{H}_{\mathrm{DC}}(P)), \quad \dot{P} = \operatorname{Ln}(\partial\mathscr{H}_{\mathrm{SP}}(P)),$$

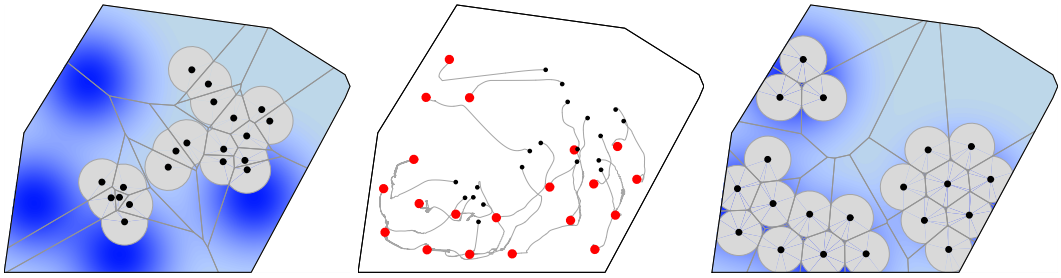

FIGURE 3. Area scenario: continuous-time algorithm (6c) for 20 mobile agents in the same convex polygonal environment and with the same density function ϕ as in Figure 1. Each agent operates with a finite sensing/communication radius equal to $r = .4$. The left (respectively, right) figure illustrates the initial (respectively, final) locations and Voronoi partition. The central figure illustrates the gradient ascent flow. For each agent i, the intersection $V_i \cap B_{\frac{r}{2}}(p_i)$ is plotted in light gray. After 36 seconds, the value of the multi-center function is approximately 14.141.

where $\mathrm{Ln} : 2^{\mathbb{R}^N} \to \mathbb{R}$ is the map that associates to each convex set $S \subset \mathbb{R}^N$ its least-norm element, $\mathrm{Ln}(S) = \mathrm{proj}_S(0)$. Alternatively, we may write for each $i \in \{1, \dots, n\}$,

$$\dot{p}_i = -\pi_i(\mathrm{Ln}(\partial \mathscr{H}_{\mathrm{DC}})(p_1, \dots, p_n)), \tag{7a}$$

$$\dot{p}_i = \pi_i(\mathrm{Ln}(\partial \mathscr{H}_{\mathrm{SP}})(p_1, \dots, p_n)), \tag{7b}$$

where $\pi_i : (\mathbb{R}^2)^n \to \mathbb{R}^2$ is the canonical projection onto the ith factor. Note that the vector fields (7a) and (7b) are discontinuous, and therefore, we understand its solution in the Filippov sense [18]. One needs to first compute the generalized gradients at P, $\partial \mathscr{H}_{\mathrm{DC}}(P)$ and $\partial \mathscr{H}_{\mathrm{SP}}(P)$, then compute the least-norm element, and finally project to each of the n components. Note that the least-norm element of convex sets can be computed efficiently, see [26], however closed-form expressions are not available in general. One can also see that the compact set Q^n is strongly invariant for both vector fields $-\mathrm{Ln}(\partial \mathscr{H}_{\mathrm{DC}})$ and $\mathrm{Ln}(\partial \mathscr{H}_{\mathrm{SP}})$ (cf. [21]).

Proposition 4.3 *For the dynamical system* (7a) *(respectively* (7b)*), the generators' location $P = (p_1, \dots, p_n)$ converges asymptotically to the set of critical points of $\mathscr{H}_{DC}$ (respectively, $\mathscr{H}_{SP}$).*

The gradient dynamical systems (7a) and (7b) enjoy the convergence guarantees stated in Proposition 4.3, but their implementation is not spatially distributed over the Delaunay graph $\mathscr{G}_{\mathrm{D}}$ because of two reasons. First, the values of all functions G_i (respectively F_i) need to be compared in order to determine which generators are active. Second, the least-norm element of the generalized gradients depends on the relative position of the active generators with respect to each other and to the environment. This is the reason why in what follows we propose a distributed implementation of the previous gradient dynamical systems and explore their relation with behavior-based rules.

Consider the following variations of the gradient dynamical systems in equation (7),

$$\dot{p}_i = -\mathrm{Ln}(\partial \lg_{V_i(P)})(P), \tag{8a}$$

$$\dot{p}_i = \mathrm{Ln}(\partial \,\mathrm{sm}_{V_i(P)})(P), \tag{8b}$$

for $i \in \{1,\dots,n\}$. Note that the systems (8a) and (8b) are spatially distributed over the Delaunay graph $\mathcal{G}_{\mathrm{D}}$, since $\mathrm{Ln}(\partial \lg_{V_i(P)})(P)$ is determined only by the position of p_i and of its Voronoi neighbors $\mathcal{N}_{\mathcal{G}_{\mathrm{D}},p_i}(P)$, and $\mathrm{Ln}(\partial \mathrm{sm}_{V_i(P)})(P)$ is determined only by the position of p_i and its nearest neighbors (which, in particular, must be Voronoi neighbors). As for the previous dynamical systems, note that these vector fields are discontinuous, and therefore, we understand its solutions in the Filippov sense. One can see that the compact set Q^n is strongly invariant for both vector fields. Moreover, for $P \in Q^n$, the solutions of the dynamical systems (8a) and (8b) starting at P are unique. The following statement summarizes the results concerning these dynamical systems (for the notion of weakly invariant set, we refer to [18, 19]).

Proposition 4.4 *Consider the dynamical systems on Q^n defined by equations* (8a) *and* (8b) *for the multi-center functions $\mathcal{H}_{DC}$ and $\mathcal{H}_{SP}$. Then, we have*

(i) Both dynamical systems are spatially distributed over the Delaunay graph $\mathcal{G}_{\mathrm{D}}$.

(ii) For the dynamical system (8a) *(resp. the dynamical system* (8b)*), the generators' location $P = (p_1,\dots,p_n)$ converges asymptotically to the largest weakly invariant set contained in the closure of $A_{\mathrm{DC}}(Q) = \{P \in Q^n \mid$ i such that $G_i(P) = \mathcal{H}_{DC}(P) \implies p_i = \mathrm{CC}_{V_i}\}$ (resp. the largest weakly invariant set contained in the closure of $A_{\mathrm{SP}}(Q) = \{P \in Q^n \mid$ i such that $F_i(P) = \mathcal{H}_{SP}(P) \implies p_i \in \mathrm{IC}_{V_i}\}$).*

Remarks 4.5 (Relation with behavior-based robotics) The dynamical systems (8a) and (8b) have an interesting connection with basic interaction laws in behavior-based robotics.

Move toward the furthest-away vertex: Consider the distributed gradient control law in the disk-covering setting (8a). For the ith generator, if the maximum of $\lg_{V_i(P)}$ is attained at a single vertex v of its Voronoi cell V_i, then (at fixed $V_i(P)$) $\lg_{V_i(P)}$ is differentiable at that configuration, and its derivative corresponds to versus$(p_i - v)$. Therefore, the control law (8a) corresponds to the behavior "move toward the furthest vertex in own Voronoi cell." If there are two or more vertexes of V_i where the value $\lg_{V_i(P)}(p_i)$ is attained, then (8a) provides an average behavior by computing the least-norm element in the convex hull of all versus$(p_i - v)$ such that $\|p_i - v\| = \lg_{V_i(P)}(p_i)$.

Move away from the nearest neighbor Consider the distributed gradient control law in the sphere-packing setting (8b). For the ith generator, if the minimum of $\mathrm{sm}_{V_i(P)}$ is attained at a single edge e, then (at fixed $V_i(P)$) $\mathrm{sm}_{V_i(P)}$ is differentiable at that configuration, and its derivative is n_e. The control law (8b) corresponds to the behavior "move away from the nearest neighbor" (where a neighbor can also be the boundary of the environment). If there are two or more edges where the value $\mathrm{sm}_{V_i(P)}(p_i)$ is attained, then (8b) provides an average behavior in an analogous manner as before.

One could also consider other distributed dynamical systems that also optimize the multi-center functions $\mathcal{H}_{\mathrm{DC}}$ and $\mathcal{H}_{\mathrm{SP}}$, based on the idea of geometric centering. Roughly

speaking, each agent moves toward the circumcenter of its own Voronoi region, for the worst-case scenario, and toward the incenter of its own Voronoi region, for the non-interference scenario. These strategies are the counterparts of the "move toward the centroid" law in equation (6a) for the expected value scenario. They also enjoy similar convergence properties to those of the dynamical systems (8a) and (8b). A detailed discussion can be found in [21].

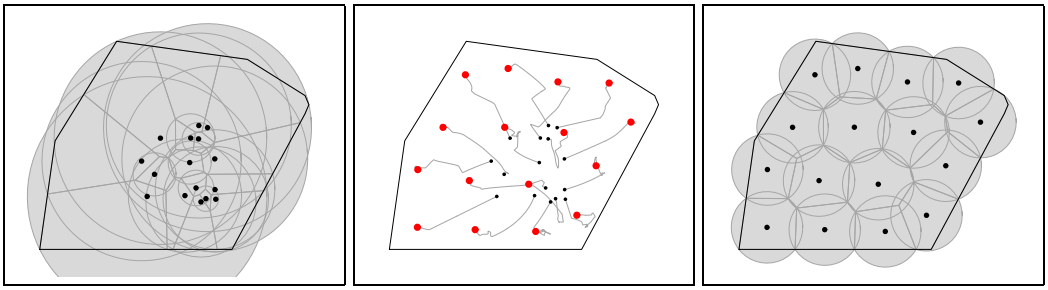

FIGURE 4. Worst-case scenario: "move-toward-the-furthest-away-vertex" algorithm for 16 mobile agents in a convex polygonal environment determined by the vertexes with coordinates $\{(0,0),(2.5,0),(3.45,1.5),(3.5,1.6),(3.45,1.7),(2.7,2.1),(1.,2.4),(.2,1.2)\}$ (in meters). The left (respectively, right) figure illustrates the initial (respectively, final) locations and Voronoi partition. The central figure illustrates the network evolution. After 2 sec., the value of the multi-center function $\mathscr{H}_{\text{DC}}$ is approximately .39504 m.

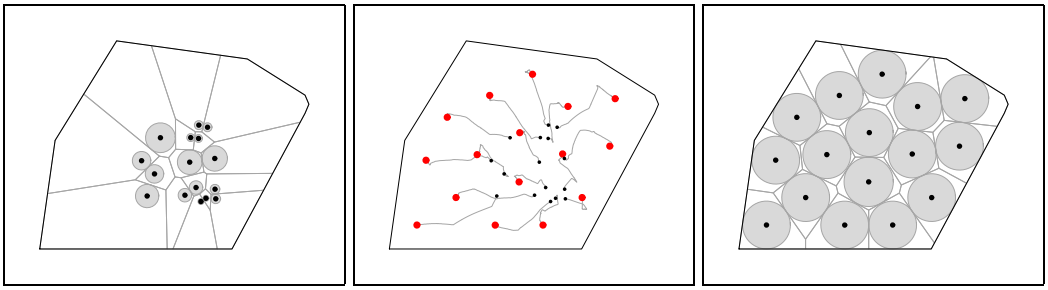

FIGURE 5. Non-interference scenario: "move-away-from-closest-neighbor" algorithm for 16 mobile agents in the same convex polygonal environment as in Figure 4. The left (respectively, right) figure illustrates the initial (respectively, final) locations and Voronoi partition. The central figure illustrates the network evolution. After 2 sec., the value of multi-center function $\mathscr{H}_{\text{SP}}$ is approximately .26347 m.

ACKNOWLEDGMENTS

This material is based upon work done in joyful collaboration with Francesco Bullo and Sonia Martínez. The author thanks the organizers of the International Workshop on Global Analysis for the warm hospitality throughout the meeting and the opportunity to present this work. The partial support by NSF SENSORS Award IIS-0330008 is gratefully acknowledged.

REFERENCES

1. Reynolds, C. W., *Computer Graphics*, **21**, 25–34 (1987).
2. Okubo, A., *Advances in Biophysics*, **22**, 1–94 (1986).
3. Arkin, R. C., *Behavior-Based Robotics*, Cambridge University Press, Cambridge, UK, 1998, ISBN 0262011654.
4. Ando, H., Oasa, Y., Suzuki, I., and Yamashita, M., *IEEE Transactions on Robotics and Automation*, **15**, 818–828 (1999).
5. Jadbabaie, A., Lin, J., and Morse, A. S., *IEEE Transactions on Automatic Control*, **48**, 988–1001 (2003).
6. Passino, K. M., *Biomimicry for Optimization, Control, and Automation*, Springer Verlag, New York, NY, 2004, in print.
7. Cortés, J., Martínez, S., Karatas, T., and Bullo, F., *IEEE Transactions on Robotics and Automation*, **20**, 243–255 (2004).
8. Ögren, P., Fiorelli, E., and Leonard, N. E., *IEEE Transactions on Automatic Control* (2004), to appear.
9. Olfati-Saber, R., and Murray, R. M., *IEEE Transactions on Automatic Control* (2003), to appear.
10. Lin, J., Morse, A. S., and Anderson, B. D. O., "The multi-agent rendezvous problem: an extended summary," in *Proceedings of the 2003 Block Island Workshop on Cooperative Control*, edited by N. E. Leonard, S. Morse, and V. Kumar, Lecture Notes in Control and Information Sciences, Springer Verlag, New York, NY, 2004, to appear.
11. de Berg, M., van Kreveld, M., and Overmars, M., *Computational Geometry: Algorithms and Applications*, Springer Verlag, New York, NY, 1997, ISBN 354061270X.
12. Okabe, A., Boots, B., Sugihara, K., and Chiu, S. N., *Spatial Tessellations: Concepts and Applications of Voronoi Diagrams*, Wiley Series in Probability and Statistics, John Wiley & Sons, New York, NY, 2000, second edn., ISBN 0471986356.
13. Agarwal, P. K., and Sharir, M., *ACM Computing Surveys*, **30**, 412–458 (1998).
14. Boltyanski, V., Martini, H., and Soltan, V., *Geometric methods and optimization problems*, vol. 4 of *Combinatorial optimization*, Kluwer Academic Publishers, Dordrecht, The Netherlands, 1999, ISBN 0792354540.
15. Drezner, Z., editor, *Facility Location: A Survey of Applications and Methods*, Springer Series in Operations Research, Springer Verlag, New York, NY, 1995, ISBN 0-387-94545-8.
16. Du, Q., Faber, V., and Gunzburger, M., *SIAM Review*, **41**, 637–676 (1999), ISSN 1095-7200.
17. Clarke, F. H., *Optimization and Nonsmooth Analysis*, Canadian Mathematical Society Series of Monographs and Advanced Texts, John Wiley & Sons, 1983, ISBN 0-471-87504-X.
18. Filippov, A. F., *Differential Equations with Discontinuous Righthand Sides*, vol. 18 of *Mathematics and Its Applications*, Kluwer Academic Publishers, Dordrecht, The Netherlands, 1988.
19. Bacciotti, A., and Ceragioli, F., *ESAIM. Control, Optimisation & Calculus of Variations*, **4**, 361–376 (1999).
20. Shevitz, D., and Paden, B., *IEEE Transactions on Automatic Control*, **39**, 1910–1914 (1994).
21. Cortés, J., and Bullo, F., *SIAM Journal on Control and Optimization* (2003), to appear.
22. Cortés, J., Martínez, S., and Bullo, F., *ESAIM. Control, Optimisation & Calculus of Variations* (2004), submitted.
23. Jaromczyk, J. W., and Toussaint, G. T., *Proceedings of the IEEE*, **80**, 1502–1517 (1992).
24. Lynch, N. A., *Distributed Algorithms*, Morgan Kaufmann Publishers, San Mateo, CA, 1997, ISBN 1558603484.
25. Suzuki, A., and Drezner, Z., *Location Science*, **4**, 69–82 (1996).
26. Boyd, S., and Vandenberghe, L., *Convex Optimization*, Cambridge University Press, Cambridge, UK, 2004, ISBN 0521833787.